GEO SATELLITES' MANUFACTURING MARKERS FROM PHOTOMETRIC COLORS

Alessandra Di Cecco[1], Alberto Buzzoni[2], Maddalena Mochi[3], Giuseppe Altavilla[4,5], Sara Brambilla[6], Marco Castronuovo[1], Fiore De Luise[7], Silvia Galleti[2], José Guichard[8], Cosimo Marzo[1], Gaetano Valentini[7]

[1]ASI, Italian Space Agency, via del Politecnico snc, Rome, IT,
E-mail: alessandra.dicecco@asi.it, marco.castronuovo@asi.it, cosimo.marzo@asi.it
[2]INAF, OAS Osservatorio di Astrofisica e Scienza dello Spazio, via Gobetti 93/3, Bologna, IT,
E-mail: alberto.buzzoni@inaf.it , silvia.galleti@inaf.it
[3]Università degli Studi di Pisa, Largo Pontecorvo, Pisa, IT,
E-mail: maddalena.mochi@phd.unipi.it
[4]SSDC-ASI, via del Politecnico snc, Rome, IT,
E-mail: giuseppe.altavilla@ssdc.asi.it
[5]INAF, OAR Osservatorio Astronomico di Roma, Via Frascati 33, I-00078 Monte Porzio Catone (RM), IT,
E-mail: giuseppe.altavilla@inaf.it
[6]Aero Club Monte Cornizzolo, Via San Miro 10, Suello (LC), IT
[7]INAF, OAAB Osservatorio Astronomico d'Abruzzo, via Mentore Maggini snc, Teramo, IT,
E-mail: fiore.deluise@inaf.it, gaetano.valentini@inaf.it
[8]INAOE, Instituto Nacional de Astrofísica, Óptica y Electrónica, L.E. Erro 1, Tonantzintla, Puebla, 72840 (México),
Email: jguich@inaoep.mx

ABSTRACT

We present the photometric analysis of 23 GEO satellites. Our dataset consists of more than 1,200 images collected by three optical telescopes, located in different observational sites, by using the Johnson-Cousin photometric filters (BVRI). The observational strategy we adopted is based on alternating the V-R-I filter-sequence, thus obtaining consecutive multi-band images, in order to reduce the color-indexes uncertainty. We reconstruct the color-color planes obtaining that the satellites' bus model and the dry mass seem to significantly affect the V-I color index.

Keywords: GEO, photometry, lightcurve
2010 MSC: 00-01, 99-00

1 INTRODUCTION

Since the beginning of the space exploration history, in the sixties, thousands of launches have been carried out, putting in orbit more than 10,000 satellites [1]. Apart from the undoubted technological leap in the use of space infrastructures for different purposes, a side effect has been represented by the proliferation of a significant amount of space debris. Beyond the increasing interest in studying this class of objects, the space debris population is far from being completely known and many efforts have still to be done. To this purpose, both optical and radar observations are widely used to study orbits, surface materials, rotation and shape of space debris. In particular, the multi-bands optical photometry is proving extremely useful to characterize the object's materials [2, 3, 4] and components [5, 6], especially by comparing

observational color-color planes and homologous laboratory measurements [7, 8]. Different photometric systems have also been used for physical characterization of space debris, such as the (BVRI) Johnson-Cousins [9, 10, 11, 3], the SDSS/Sloan (g'r'i'z') [12], and the infrared bands [13]. By using a sample of 61 geostationary (GEO) satellites, the recent investigation by Schmitt (2020, [14]) highlights how the photometric colors are an important tool in the identification of satellites manufacturers and bus configuration (i.e. shape, size, antennae, solar array, etc.).

In this paper we present a multi-color photometry investigation of 23 satellites located along the Clarke Belt and active at the time of the observations. In particular, we present the analysis and the results obtained by using more than 1,200 multi-band images, focussing on the possible correlation between the photometric color-indexes and the satellites bus configuration, referring to and increasing Schmitt's sample.

2 OBSERVATIONAL DATASET

The observational datasets were collected by using three ground-based telescopes, each equipped with Johnson-Cousins photometric system's bands. Two telescopes, the Cassini-Loiano and the Teramo-Normale-Telescope (TNT) are located in Italy, belonging to the National Institute for Astrophysics (INAF); while, the third telescope belongs to the Guillermo Haro Astrophysical Observatory (GHAO) and is located in Cananea, Mexico. The Cassini-Loiano telescope has a Ritchey-Chrétien configuration and mounts a Charge-Coupled-Device (CCD) camera of 1300x1340 pixels, with a pixel scale of 0.58 arcsec/pixel and a total Field-of-View (FoV) of 13'x12.6' arcmin. By using this telescope, we carried out an observational campaign, from August 2010 to April 2011, observing 11 GEO satellites with B, V and I filters. The TNT telescope is equipped with a CCD camera of 1024X1024 pixels, with a pixel scale of ≈0.3 arcsec/pixel and a FoV of ≈5x5 square arcminutes ([15]). In 2017, the TNT was used to collect multi-band photometric data of 8 GEO satellites, by using the V, R and I filters. The Cananea telescope was used to collect B, V and R images for 4 GEO satellites in 2015.

The observed objects are listed in Tab. 1. For each satellite, from 30 to 60 images were analysed and the entire dataset consists of more than 1,200 scientific frames.

During each night, we observed several reference stars by using the Landolt (1992, [16]) standard fields. We also collected instrumental calibration frames to consider the flat-field and electronic bias contributions, while the dark current was negligible. In order to analyse the data, we processed the images developing automatic reduction pipelines, by using the IRAF[1] software [17]. After the correction for the instrumental calibration frames, we applied the aperture photometry technique, obtaining the absolute magnitude of the GEO objects thanks to Landolt's standards. Taking into account the uncertainties related to the photometric analysis and the calibration procedures, we estimated a magnitude error of $V \approx 0.26$, $R \approx 0.23$ and $I \approx 0.22$ mag.

By inspecting the scientific images, we found that each satellite presents a high signal-to-noise ratio (S/N) when compared to the sky background (S/N >>1000).

[1] Image Reduction and Analysis Facility, a general purpose software system for the reduction and analysis of astronomical data, written by the National Optical Astronomy Observatories (NOAO) in Tucson, Arizona. However, development and maintenance of IRAF is discontinued since 2013. See https://iraf-community.github.io/

Several observed targets belong to GEO satellite constellations and, for some of them, a cross-tag problem among the members occurs. For instance, we show this issue for the ASTRA GEO cluster in Fig. 1 (by using a cropped image of 10 s taken with the R band of the Cassini telescope). In this case, the cluster of four satellites in GEO orbit clearly appears in the observations (left panel of Fig. 1) and closely matches the expected location according to up-to-date NORAD TLE (right panel of Fig.1). To a closer analysis, however, as far as the cluster pattern is concerned, we observed an apparent interchange between the location of ASTRA 1L and that of ASTRA 1M. Moreover, the entire cluster appears to spread over a smaller distance (≈5'20") with respect to the expected map (≈6'37") obtained from the TLE. Only a supplementary comparison of the apparent motion and colors allowed us to firmly disentangle the identification problems.

Table 1. Observed satellites list

Object	NORAD	COSPAR	Date	Observatory
ASTRA 2E	39285	2013-056A	May, 2017	Teramo, IT
ASTRA 2F	38778	2012-051A	March, 2017	Teramo, IT
ASTRA 2G	40364	2014-089A	March, 2017	Teramo, IT
EUTELSAT 21B	38992	2012-062B	May, 2017	Teramo, IT
EXPRESS AM7	40505	2015-012A	March, 2017	Teramo, IT
EXPRESS AM8	40895	2015-048A	May, 2017	Teramo, IT
TURKSAT 4A	39522	2014-007A	May, 2017	Teramo, IT
TURKSAT 4B	40984	2015-060A	May, 2017	Teramo, IT
ANIK F1R	28868	2005-036A	2015	Cananea, MX
ANIK F1	26624	2000-076A	2015	Cananea, MX
ANIK G1	39127	2013-014A	2015	Cananea, MX
MEXSAT 3	39035	2012-075B	2015	Cananea, MX
ASTRA 1H	25785	1999-033A	Aug, 2010 – Apr, 2011	Loiano, IT
ASTRA 1KR	29055	2006-012A	Aug, 2010 – Apr, 2011	Loiano, IT
ASTRA 1L	31306	2007-016A	Aug, 2010 – Apr, 2011	Loiano, IT
ASTRA 1M	33436	2008-057A	Aug, 2010 – Apr, 2011	Loiano, IT
HISPASAT 136W1 (1C)	26071	2000-007A	Aug, 2010 – Apr, 2011	Loiano, IT
HISPASAT 30W4 (1D)	27528	2002-044A	Aug, 2010 – Apr, 2011	Loiano, IT
SPAINSAT	28945	2006-007A	Aug, 2010 – Apr, 2011	Loiano, IT
EUTELSAT 13A (HOTBIRD6)	27499	2002-038A	Aug, 2010 – Apr, 2011	Loiano, IT
EUTELSAT 13B (HOTBIRD8)	29270	2006-032A	Aug, 2010 – Apr, 2011	Loiano, IT
EUTELSAT 13C (HOTBIRD9)	33459	2008-065A	Aug, 2010 – Apr, 2011	Loiano, IT
METEOSAT 8 (MSG1)	27509	2002-040B	Feb-Apr, 2011	Loiano, IT

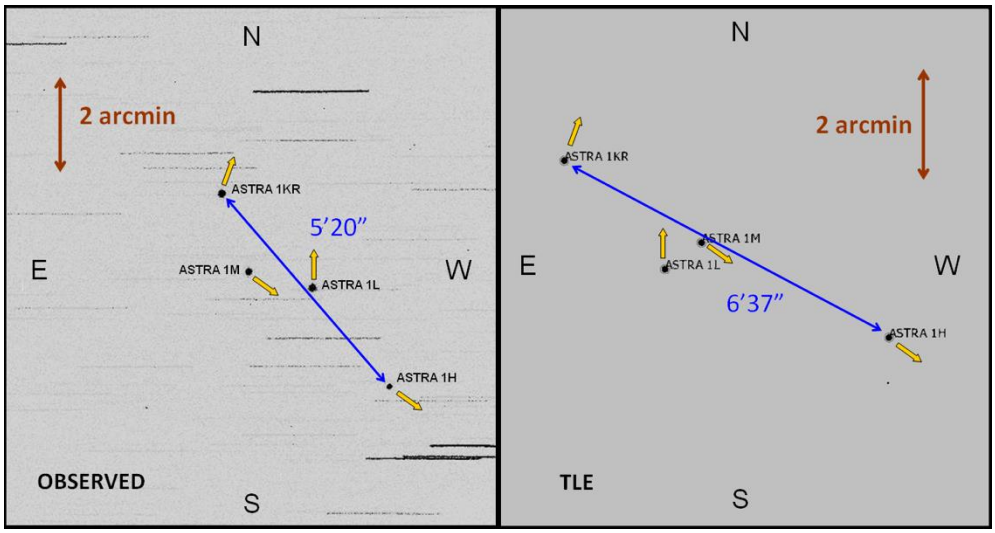

Figure 1. Cross-tag problem for ASTRA GEO constellation (yellow arrows mark apparent satellite motion).

3 PHOTOMETRIC COLOR ANALYSIS

3.1 Color-lightcurves

A multi-band photometric analysis facilitates the satellite characterization, in terms of size, structure and surface material investigation [2, 3, 4]. For instance, the photometric color-color planes seem to be a promising tool to study the bus configuration [14]. However, the observed magnitude of the GEO satellites is widely affected by the Solar phase-angle and by operational manoeuvres, as shown by several theoretical [18], observational [19] and laboratory studies [7, 20]. Therefore, the satellite magnitude changes in time and, in case of multiple observations, it is usually referred to its averaged value. As a consequence, the photometric color-indexes (B-V, V-R, V-I) reconstructed by using the mean magnitudes suffer from several uncertainties.

To address this problem, during our observational campaigns, we adopted the strategy to collect consecutive images - with an exposure time of 60 s each - by alternating the filter sequence. With this approach we were able to calculate the color-index by minimizing the time interval using two consecutive images (or the closest acquisitions in time) in two different filters. Then, we reconstructed the color-lightcurves and calculated their mean values to obtain a statistically robust estimate of the color-indexes, reducing the uncertainties with respect to the traditional approach. As instance, we show the case of ASTRA 2G in Fig. 2. For this satellite we analysed more than 20 images for each filter (VRI), obtaining three light-curves spanning approximately 0.5 mag in almost two hours of observations (top panel of Fig.2). The color-indexes calculated by the mean magnitudes are: V-R = 0.5±0.4, V-I = 0.7±0.4, R-I = 0.3±0.4 mag. By reconstructing the color-lightcurves with our approach, we estimated the following values: V-R = 0.46±0.03, V-I = 0.72±0.03, R-I = 0.27±0.02 mag (bottom panel of Fig.2). As expected, the color-lightcurves show lower uncertainties. The complete sample of our targets and color indexes are listed in Tab. 2. For the entire dataset, we found that the color-indexes span the intervals $0.61 \leq$ B-V≤ 1.55, $0.18 \leq V-R \leq 0.78$ and $0.36 \leq V-I \leq 1.96$ mag.

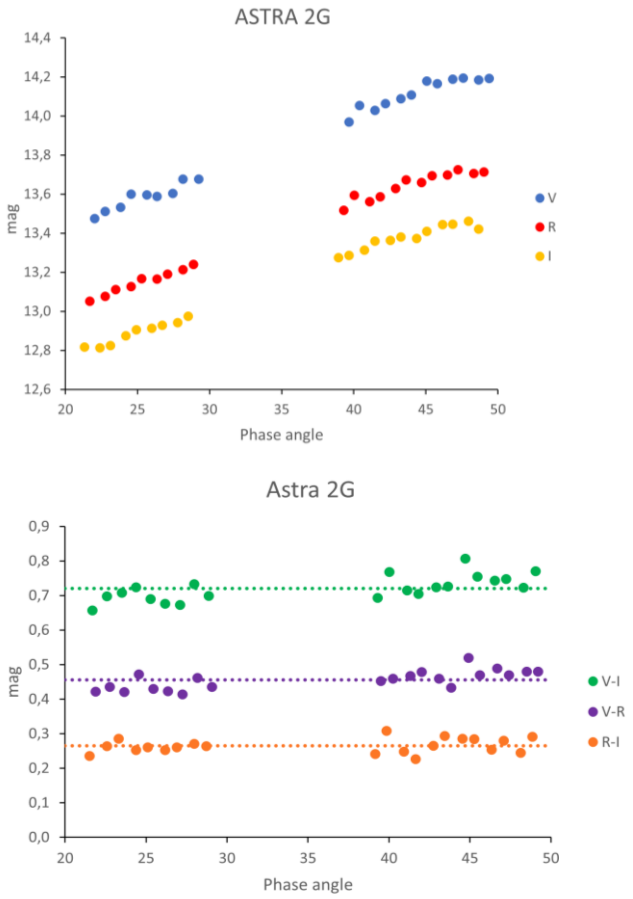

Figure 2. Lightcurves (top panel) and color-lightcurves (bottom panel) for the satellite ASTRA 2G.

Table 2. Observed satellites color-index and bus configuration.

Object	B-V	V-R	V-I	Bus configuration
ASTRA 2E		0.51	0.71	Astrium EUROSTAR-3000
ASTRA 2F		0.38	0.67	Astrium EUROSTAR-3000
ASTRA 2G		0.43	0.68	Astrium EUROSTAR-3000
EUTELSAT 21B		0.49	0.79	Alcatel SPACEBUS-4000C3
EXPRESS AM7		0.78	0.97	Astrium EUROSTAR-3000
EXPRESS AM8		0.40	0.64	ISS Reshetnev EKSPRESS-1000NTB
TURKSAT 4A		0.25	0.41	Mitsubishi MELCO DS-2000
TURKSAT 4B		0.18	0.36	Mitsubishi MELCO DS-2000
ANIK F1R	0.79	0.64		Astrium EUROSTAR-3000
ANIK F1	0.88	0.71		Hughes HS-702
ANIK G1	0.88	0.80		Loral SSL-1300
MEXSAT 3	0.61	0.60		Northrop Grumman GEOSTAR-2
ASTRA 1H	0.82		1.04	Hughes HS-601HP
ASTRA 1KR	0.73		1.05	Lockeed Martin A-2100AXS
ASTRA 1L	0.74		1.06	Lockeed Martin A-2100AXS
ASTRA 1M	1.55		1.45	Astrium EUROSTAR-3000
HISPASAT 136W1 (1C)	0.86		1.74	Alcatel SPACEBUS 3000B2
HISPASAT 30W4 (1D)	1.23		1.96	Alcatel SPACEBUS 3000B2
SPAINSAT	0.80		0.98	Loral SSL-1300
EUTELSAT 13A (HB6)	0.71		1.09	Alcatel SPACEBUS 3000B3
EUTELSAT 13B (HB8)	1.14		1.36	Astrium EUROSTAR-3000
EUTELSAT 13C (HB9)	1.25		1.24	Astrium EUROSTAR-3000
METEOSAT 8 (MSG1)	0.77		1.27	Alcatel Spin stabilized

3.2 Color-color planes

In order to investigate the correlation between the color-index and the satellite bus configuration (see Tab. 2), we used the color-color planes, plotting the color excursion of each satellite along its phase angle tracking, in panels of Fig. 3 and Fig. 4. In particular, on the V-I vs B-V color-color plane (Fig. 3), we present the satellites ASTRA 1 (H, KR, L, M, about 19°E), EUTELSAT (HOTBIRD 6, 8, 9, about 13°E), HISPASAT 1 (C, D), SPAINSAT and METEOSAT 8. We obtained that the ASTRA 1 objects clustered according to their bus structure, as shown in the top panel of Fig. 3. The ASTRA 1L and 1KR consist of a Lockheed-Martin (LM) bus architecture and they show similar colors ($0.8 \lesssim V\text{-}I \lesssim 1.2$, $0.6 \lesssim B\text{-}V \lesssim 0.9$), as well as ASTRA 1H with Boeing-Hughes (HS) bus. The ASTRA 1M satellite is based on an EUROSTAR 3000 (EU) platform and clearly sets apart presenting redder colors ($1.3 \lesssim V\text{-}I \lesssim 1.6$, $1.4 \lesssim B\text{-}V \lesssim 1.7$). The HOTBIRD satellites show a wider excursion in both colors, spanning ≈1 mag (middle panel of Fig. 3). HOTBIRD 8 and 9 have the same EU bus configuration, while HOTBIRD 6 is based on SPACEBUS 3000 (SB, bottom panel of Fig. 3).

The V-I vs V-R color-color plane shows a clusterization of the homogenous ASTRA 2 (E, F, G, 28°E) satellites, based on EUROSTAR 3000 ($0.5 \lesssim V\text{-}I \lesssim 0.9$, $0.3 \lesssim V\text{-}R \lesssim 0.6$; top panel of Fig. 4). A similar behaviour is displayed by the two Turksat 4 (A, B, 42°E and 50°E, respectively) satellites both consisting of a Melco DS-2000 bus structure ($0.3 \lesssim V\text{-}I \lesssim 0.5$, $0.1 \lesssim V\text{-}R \lesssim 0.3$, with exceedingly "blue" colors closely matching the case of an F-type star) (bottom panel of Fig. 4).

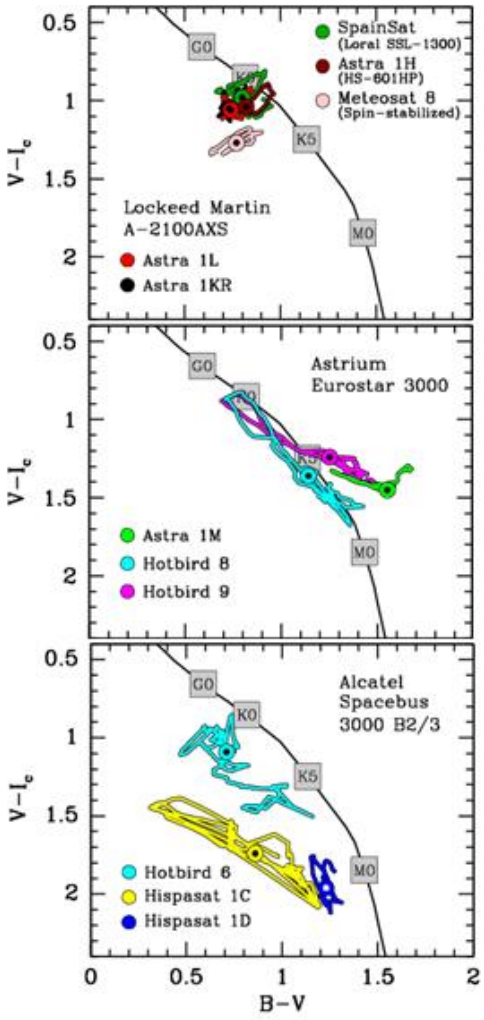

Figure 3. B-V vs. V-I color plane for our Loiano sample. Objects are grouped according to the bus architecture, as labelled top right in each panel. The color excursion of each satellite is displayed in the three panels along its phase angle tracking, marking with a dot the color at $\varphi \rightarrow 0$. Black solid line marks the stars location with spectral-type labels (grey squares).

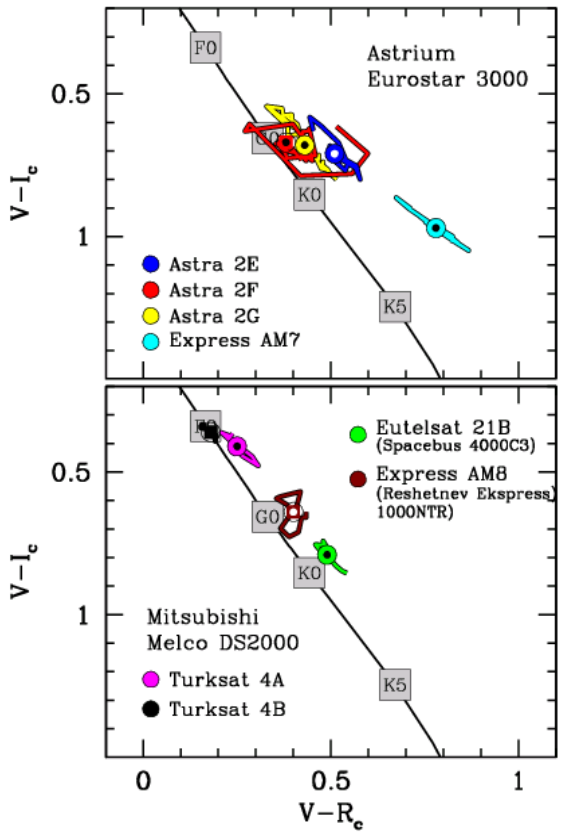

Figure 4. V-R vs. V-I color plane for our TNT satellite sample. Objects are grouped according to the bus architecture, as labelled top right in each panel. Black solid line marks the stars' location with spectral-type labels (grey squares).

3.3. Literature comparison

To compare our values with literature analysis, we plotted the color-indexes of Tab. 2 together with the results provided by Schmitt (2020, [14]), considering his mean colors calculated for different bus configurations. In the V-I vs B-V color plane, we found that common bus configurations seem occupy the same loci, with several exceptions (Fig. 5). A close agreement between our and Schmitt's results have been found for the following buses: HS, LM, Loral (LL) and THALES-Alenia Spacebus (TA). The agreement is stronger if the V-I color-index is considered, with respect to the B-V values.

We found a straight "off-track" location (bluer regions) of two SB compared to represented stellar loci. In the V-I vs V-R color plane (bottom panel of Fig. 5), we still find that similar bus configurations occupy – with several exceptions – similar areas, such as the two DS2000 (DS) of the Turksat A and B satellites, as well as the three EU of the ASTRA 2 satellites. Note the exceedingly "blue" V-R colors for the DS with respect to the entire sample. Owing to the use of different filter bands, in this color plane, a comparison between Schmitt's and our data does not provide relevant results.

Owing to the inhomogeneous datasets (that lie on different photometric filters), the color-color planes have limited statistics. However, by investigating the feature of the single color-index, we were able to include more satellites in our analysis. To this purpose, we studied the color-index considering the bus configuration, by merging our data and those from Schmitt's. In particular, we sorted this sample for the V-I, V-R and B-V color-indexes, obtaining a mild correlation between the V-I color values and the bus configuration (Fig. 6).

We singled out each bus family in order to seek out possible relations between the V-I values and age, but we did not obtain any clear evidence.

3.4 Further investigations

In order to further investigate a possible correlation between the observational data and the satellites features, we plotted the color indexes (integrating our sample with Schmitt's data, [14]) against several structural parameters (e.g. wingspan, dry mass, etc.). We found a mild correlation between the analysed color indexes and the dry mass of the observed GEO objects (Figs. 7--9).

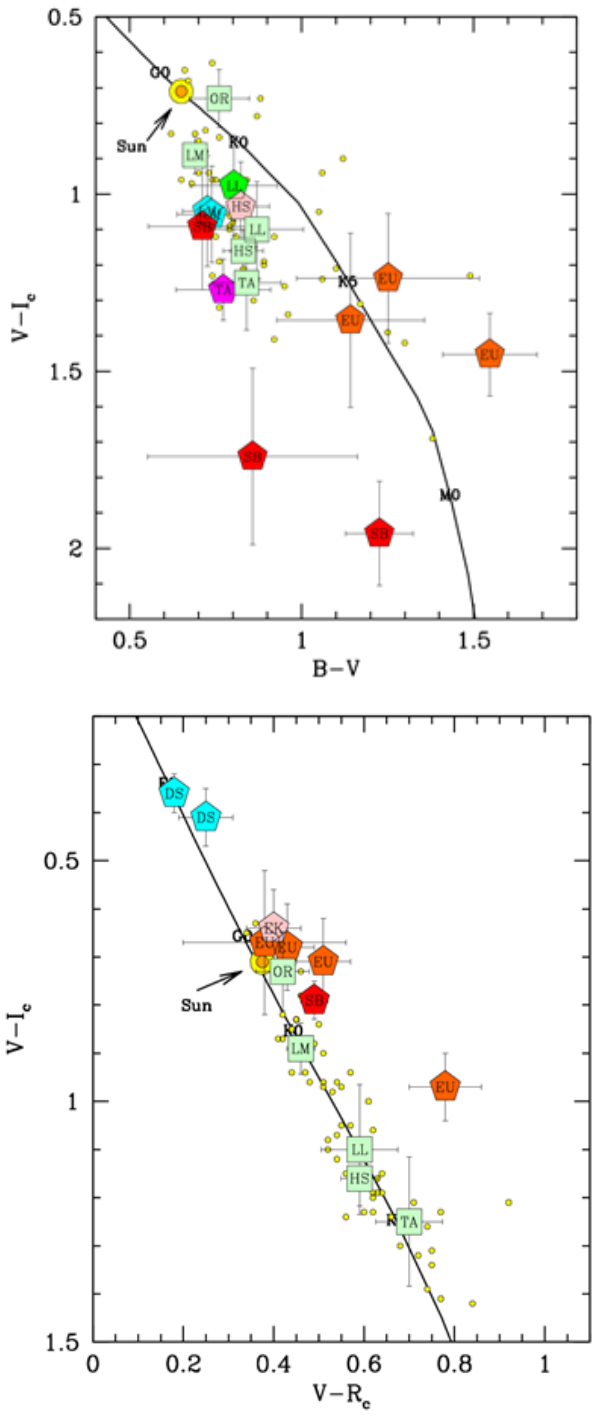

Figure 5. Color-color planes for satellites subsample comprising our (pentagons) and Schmitt's (squares) average color indexes. The bus platform acronym is shown for each satellite. Black solid line marks the stars' location.

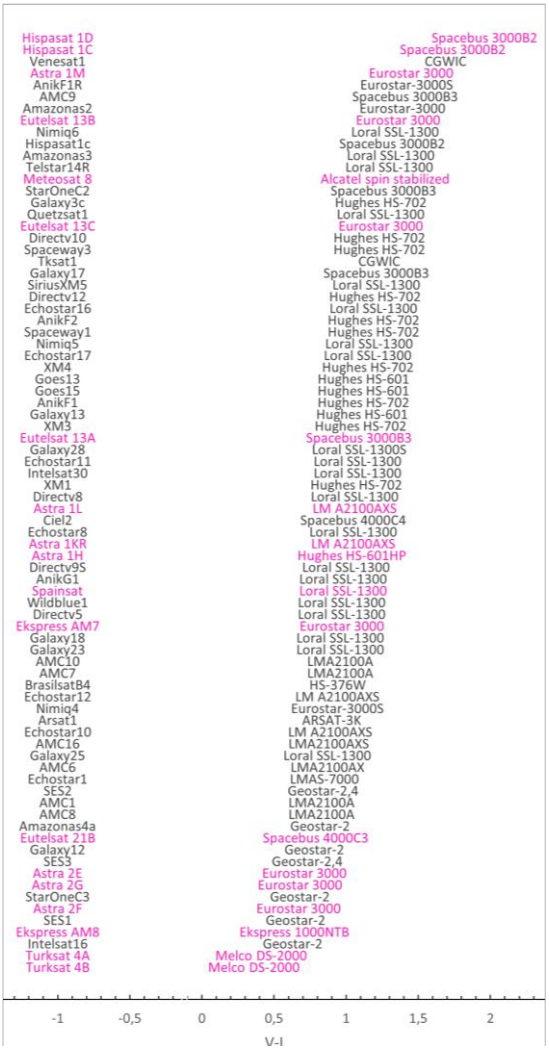

Figure 6. Sorted V-I color-index (marked by bus configuration) for satellites listed on the left. Schmitt's (2020) and our data (in pink).

4 CONCLUSIONS

In this paper, we presented the photometric analysis of a dataset of more than 1200 scientific images of GEO satellites, acquired with Johnson-Cousin bands. In particular, we reconstructed the color-lightcurves for each object and computed their mean values, thus obtaining a robust low-uncertainty estimate for the color indexes. By integrating our data with Schmitt's (2020,

[14]) sample and using the color-color planes we observed that several satellites seem to clusterize according to their bus family and model. We further investigated this behaviour for each color-index obtaining analogous results, most evident in V-I. Moreover, we studied a possible relation between the color-indexes and the satellites' structural parameters. We obtained that lower color-indexes values occur for lower dry masses, independently from the satellite age. Further investigations are required.

ACKNOWLEDGEMENTS

This investigation was funded by the Italian Space Agency and National Institute for Astrophysics Agreement on space debris ("Detriti Spaziali - Supporto alle attivita' SST e IADC 2019-2021, Accordo n.2020-6-H.0)

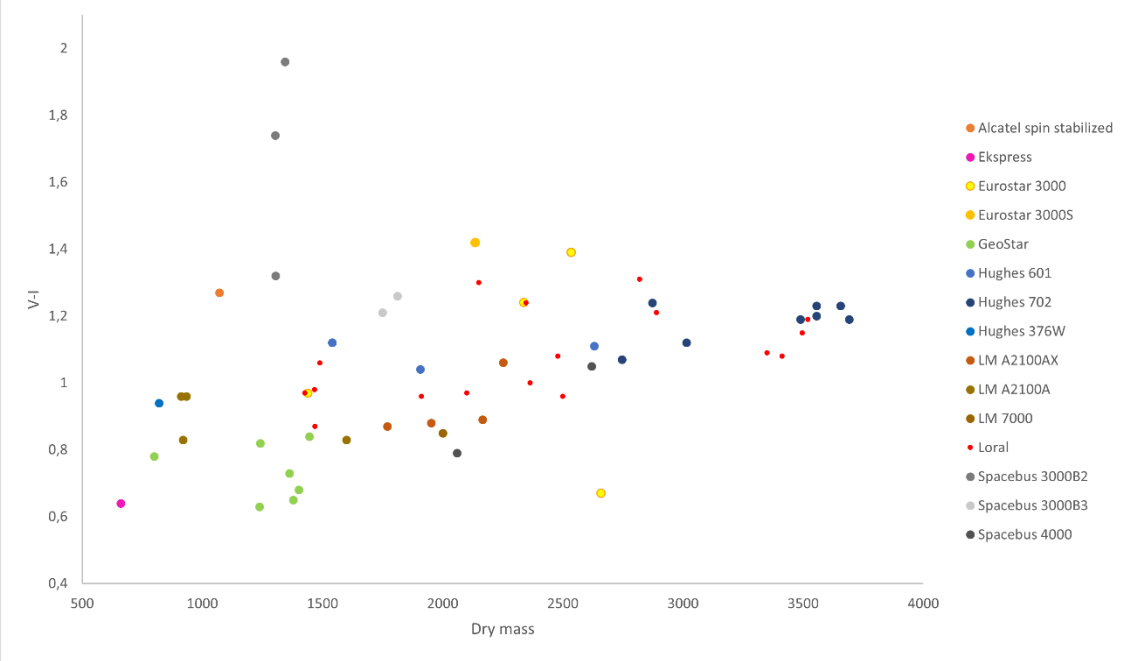

Figure 7. V-I color-index versus satellite dry mass (in kg) for different bus models.

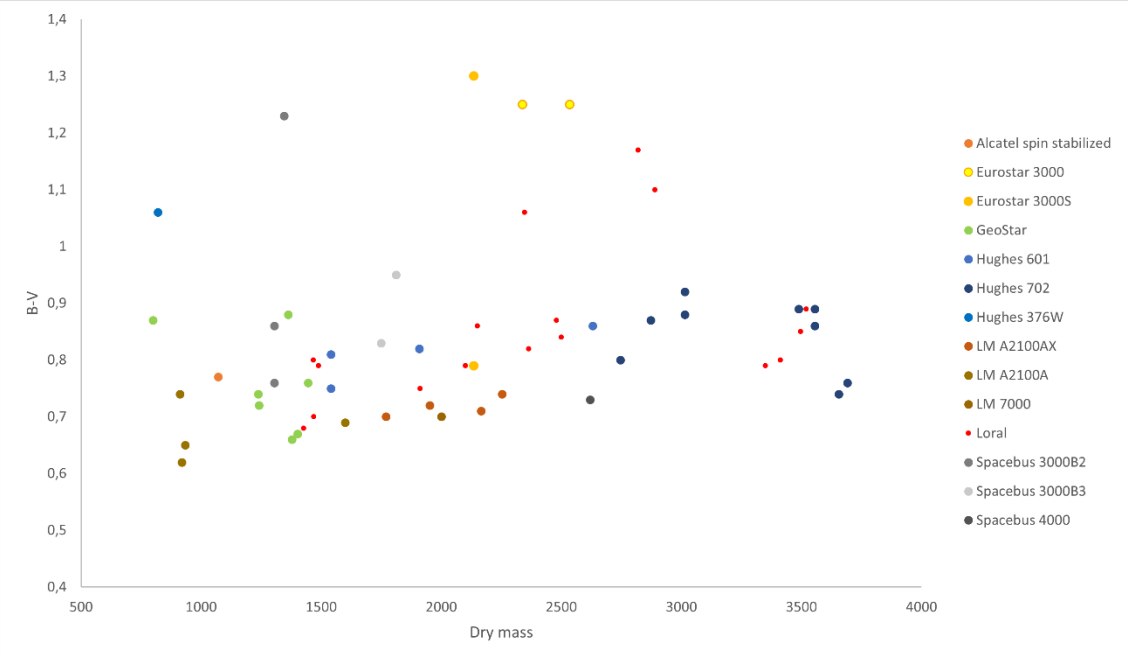

Figure 8. B-V color-index versus satellite dry mass (in kg) for different bus models.

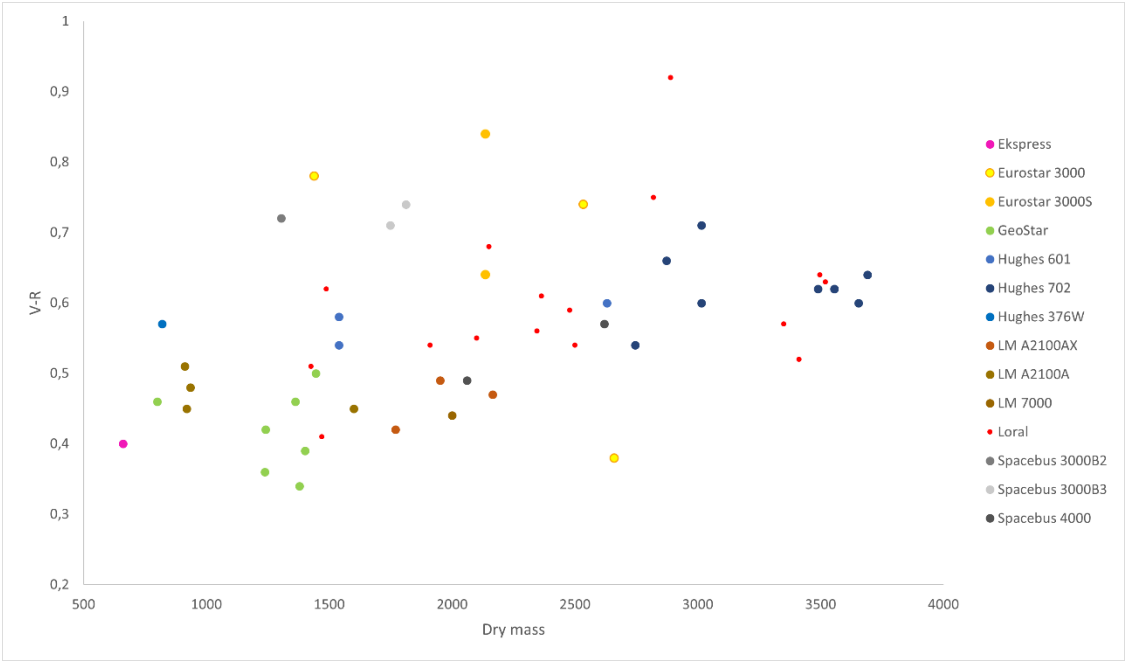

Figure 9. V-R color-index versus satellite dry mass (in kg) for different bus models.

REFERENCES

[1] ESA, "Space Environment Statistics Report," 2021.

[2] A. Vananti, T. Schildknecht e H. Krag, «Reflectance spectroscopy characterization of space debris,» *Advances in Space Research,* vol. 59, pp. 2488-2500, 2017.

[3] T. Schildknecht, R. Musci, C. Fruh e Ploner, «Color photometry and light curve observations of space debris in GEO,» in *Proceedings of Advanced Maui Optical and Space Surveillance Technologies Conference*, 2008.

[4] M. Zigo, J. Silha e S. Krajcovic, «BVRI Photometry of Space Debris Objects at the Astronomical and Geophysical Observatory in Modra,» in *Proceedings of the AMOS Meeting*, Wailea, Maui, Hawaii, 2019.

[5] D. Hall, «Surface Material Characterization from Multi-band Optical Observations,» in *Proceedings of the AMOS Meeting*, Wailea, Maui, Hawaii, 2010.

[6] X. F. Zhao, H. Y. Zhang, Y. Yu e Y. D. Mao, «Multicolor photometry of geosynchronous satellites and application on feature recognition,» *Advances in Space Research,* vol. 58, n. 11, pp. 2269-2279.

[7] H. Cowardin, P. Seitzer, K. Abercromby, E. Barker e T. Schildknecht, «Characterization of orbital debris photometric properties derived from laboratory-based measurements,» in *Proceedings of the Advanced Maui Optical and Space Surveillance Technologies Conference*, 2010.

[8] S. M. Lederer, P. Seitzer, H. Cowardin, K. Abercromby, E. Barker e A. Burkhardt, «Characterizing Orbital Debris and Spacecrafts through a Multi-Analytical Approach,» in *Proceedings of the Advanced Maui Optical and Space Surveillance Technologies Conference*, 2012.

[9] T. Cardona, P. Seitzer, A. Rossi, F. Piergentili e F. Santoni, «BVRI photometric observations and light-curve analysis of GEO objects,» *Advances in Space Research,* vol. 58, n. 4, pp. 514-527, 2016.

[10] E. Cordelli, P. Schlatter e T. Schildknecht, «Simultaneous multi-filter photometric characterization of space debris at the Swiss Optical Ground Station and Geodynamics Observatory Zimmerwald,» in *Proceedings of the Advanced Maui Optical and Space Surveillance Technologies Conference*, 2018.

[11] P. Seitzer, H. Cowardin, E. Barker, T. Abercromby, K. Kelecy e M. Horstman, «Optical Photometric Observations of GEO Debris,» in *Proceedings of the Advanced Maui Optical and Space Surveillance Technologies Conference*, 2010.

[12] Y. Lu, C. Zhang, R. Sun, C. Y. Zhao e J. N. Xiong, «Investigations of associated multi-band observations for GEO space debris,» *Advances in Space Research,* vol. 59, n. 10, pp. 2501-2511, 2017.

[13] S. M. Lederer, H. M. Cowardin, B. Buckalew, J. Frith, P. Hickson, L. Pace, M. Matney, P. Anz-Meador, P. Seitzer, E. Stansbery e T. Glesne, «NASA's Orbital Debris Optical and IR Ground-based Observing Program: Utilizing the MCAT, UKIRT, and Magellan Telescopes,» in *Proceedings of the Advanced Maui Optical And Space Surveillance Technologies Conference*, 2016.

[14] H. R. Schmitt, «Multi wavelength optical broad band photometric properties of a representative sample of geostationary satellites,» *Advances in Space Research,* vol. 65, n. 1, pp. 326-336, 2020.

[15] A. Di Cecco, F. De Luise, C. Marzo, C. Portelli, M. M. Castronuovo e G. Valentini, «Multi-band photometric observations of GEO satellites: Preliminary Results,» in *Proceedings of the 7th European Conference on Space Debris*, Darmstadt, 2017.

[16] A. U. Landolt, «UBVRI Photometric Standard Stars in the Magnitude Range 11.5 < V < 16.0 Around the Celestial Equator,» *Astronomical Journal,* vol. 104, pp. 340-371, 1992.

[17] L. E. Davis, «Stellar Photometry Tools in IRAF,» in *Precision CCD Photometry Workshop, ASP Conference Series*, 1999.

[18] J. Africano, P. Kervin, D. Hall, P. Sydney, J. Ross, T. Payne, S. Gregory, K. Jorgensen, K. Jarvis, T. Parr-Thumm, G. Stansbery e E. Barker, «Understanding Photometric Phase Angle Corrections,» in *Proceedings of the 4th European Conference on Space Debris*, Darmstadt, 2005.

[19] X. F. Zhao, Y. Yu, Y. Mao e Z. H. Tang, «Long-term photometric signature study of two GEO satellites,» *Advances in Space Research,* vol. 67, n. 8, pp. 2241-2251, 2021.

[20] J. Hostetler e H. Cowardin, «Experimentally-Derived Phase Function Approximations in Support of the Orbital Debris Program Office,» in *First International Orbital Debris Conference*, Sugar Land, Texas, 2019.

[21] M. Cathala, «The Alcatel Spacebus Family,» in *Cooperation in Space, Euro-Asian Space Week*, 1999.